A NEURO-FUZZY BASED CONTROL OF A SIMULATED SOFC IN A GRID CONNECTED ENVIRONMENT

Sohail Khan
Universidad Nacional Autónoma de México
sohailmomand6@gmail.com

Juan Carlos Olivares Galvan
UAM Azcapotzalco
jolivaresgalvan@gmail.com

Rafael Escarela-Perez
UAM Azcapotzalco
r.escarela@ieee.org

Resumen

En este trabajo de investigación, la celda de combustible de óxido sólido (SOFC), con una potencia nominal de 50 kW, está conectada con el inversor de voltaje (VSI) y la técnica de conmutación aplicada al control de corriente de histéresis. Los controladores Estándar del Modelo Aditivo (SAM) Neuro-Fuzzy y PI se emplean por separado para controlar la demanda de potencia activa y reactiva de la red. La potencia real y la potencia reactiva se controlan mediante la manipulación de las corrientes de los ejes d y q, respectivamente. Se encontró que tanto Neuro-Fuzzy como los controladores PI son capaces de controlar la demanda de potencia activa y reactiva de la red, pero la primera sustituye a la última. La tensión de salida y las formas de onda de corriente del inversor se simulan para suavizarlas y hacerlas deseables para el acoplamiento con la red. La estrategia de control desacopla la potencia real y reactiva y asegura su flujo independiente en la red. Toda la configuración se simula en MATLAB / Simulink.

Palabras Claves: Celda de combustible de óxido sólido, control Neuro-Fuzzy, modelo de aditivo estándar, control de potencia activa y reactiva.

Abstract

In this research paper, a Solid Oxide Fuel Cell (SOFC), rated at 50 kW, is interfaced with grid through Voltage Source Inverter (VSI) and switching technique applied is Hysteresis Current Control. Standard Additive Model (SAM) based Neuro-Fuzzy and PI controllers are separately employed to control the Active and Reactive power demand of grid. The real and reactive powers are controlled by the manipulation of d and q axis currents, respectively. It was found that both Neuro-Fuzzy and PI controllers are capable in controlling the demand Active and Reactive powers of grid but the former supersede the latter. The output voltage and current waveforms of the inverter are simulated for smoothness in order to make it desirable for coupling with the grid. The control strategy decouples the real and reactive power and ensures their independent flow in the grid. The whole setup is simulated in MATLAB/Simulink.

Keywords*: *Active and Reactive power control, Neuro-Fuzzy Control, solid Oxide Fuel Cell, standard Additive Model.

1. Introduction

Neo-liberal market and environmental concern have convinced the utilities and researchers at the global level to exploit the technologies which are less expensive, efficient, and environment friendly. The introduction of the Distributed Generation (DG) systems powered by the fuel cells, micro turbines and photovoltaic cells are among the steps towards this end. These DG systems are gaining popularity due to their high operating efficiency, improved reliability and a lower emission of harmful gasses. An enhanced efficiency and power quality even in peak-loads has attracted the customers. On the other hand, the utilities are served by alleviating the cost required for the installation of new transmission lines. Hence, both the utilities and end-users are benefited by DG [Asadi et al., 2014] [Khan, 2015].

The demand for the renewable energy is increasing due to the increasing need of electrical energy. The benefits like: environmental friendliness, reduction of transmission losses, peak load shaving, and it’s utility as backup sources further compliment the usefulness of the renewable energy resources [Kang et al., 2011]. Among several DG sources, fuel cells are generally conceived compatible as these are modular and having high efficiency with no harmful emissions [Vaishampayan et al., 2014].

The time-varying grid demand and withdrawal of reactive power from the generating system certainly affect the current and voltage waveforms and causes the harmonics behavior. This research paper aims to satisfy the time-varying grid demand while removing the harmonics from the voltage waveform. The D Q control strategy is implemented using two controllers (PI and SAM based Neuro-Fuzzy, separately) and their performance are evaluated on the basis of tracking time.

SOFC is a device which converts chemical energy of hydrogen into electric power. Among different types of fuel cells, it has a very high operating temperature which enlists SOFC in the most favorable technologies especially for stationary applications. Also, there is no need of a precious metal as a catalyst. The solid state electrolyte of SOFC adds some distinct qualities to it. Unlike other fuel cells, the stack of SOFC does not have to be fabricated in plate like configuration. In comparison with Molten Carbonate Fuel Cells (MCFC), it has a very low corrosion with no water management issues as in PEMFC [Mekhilef et al., 2012]. It can be operated on variety of fuels other than hydrogen because it can re-form the fuel internally.

The reactions take place in the system are given bellow,

$$H_2 + O_2 \dashrightarrow H_2O + 2e$$

$$CO + O_2 \dashrightarrow CO_2 + 2e$$

While the reaction take place at anode is given bellow,

$$O_2 + 4e \rightarrow 2O^{2-}$$

The overall reaction can be presented as,

$$H_2 + O_2 + CO \rightarrow HO_2 + CO_2$$

In this section, mathematical modeling of SOFC has been given. The model is based on the Nernest's equation. The following assumptions have been made while developing this model:

- No loss of gases.
- The temperature of SOFC is constant

Considering the losses such as, ohmic loss, concentration loss and activation loss, the stack output voltage can be written as equation 1 [Bhuyan, 2011].

$$V_{dc} = V_0 - rI - \eta_{act} - \eta_{con} \tag{1}$$

Where, V_0 represents the open-circuit reversible potential in volts, r represents resistance in ohms and I is the current in amperes, η_{act} is activation drop in volts, and η_{con}represents the losses due to concentration in volts.

The behavior of SOFC is defined by Nernest's equation given bellow, equation 2.

$$V_0 = N_0\left[E^0 + \frac{RT^0}{2F}\ln\frac{x_{H_2}x_{O_2}x_{O_2}^{\frac{1}{2}}}{x_{H_2O}}\right] \tag{2}$$

In the equation 2, E^0 represents the standard reversible cell potential, x_i is the mole fraction of species, F is Faraday's constant in Coulomb per kilo mole, T represents the stack temperature in Kelvin, and $N_0$is the number of cells present in the stack.

Rest of the paper is organized in the following manner. In section 2, SOFC is discussed followed by section 3 with its dynamic modeling. In section 4, the power conditioning unit is explained followed by section 5, in which the control strategy is discussed. Neuro-fuzzy controller is presented with its respective modeling in section 6. The simulation results and conclusion are given in section 7 and 8 respectively.

2. Methods

Power Conditioning Unit Model

The voltage source inverter (VSI) and Hysteresis Current Control forms the power conditioning unit. This unit performs the control action and transforms the DC output of the SOFC into AC.

The VSI is directly connected to convert the fuel cell direct voltage into alternating thus alleviating the cost and reducing the loss associated with the DC/DC converter. This is achieved by using the hysteresis current control technique where a power switch is operated at a high frequency.

The mathematical representation of output voltage with modulation index being a domain is modeled as equation 3.

$$V_{ac} = mV_{cell}\angle\delta \tag{3}$$

While real and reactive power are as equations 4 y 5.

$$P_{ac} = \frac{mV_{cell}V_s}{X}\sin\delta \tag{4}$$

$$Q = \frac{(mV_{cell})^2 - mV_{cell}V_s\cos\delta}{X} \tag{5}$$

In the expressions 3, 4 and 5, V_{ac} represents the alternating voltage, m represents the modulation index of the inverter, δ is the phase angle, P_{ac} and Q are the AC output active and reactive power from the inverter, respectively. V_s represents the terminal voltage , and X is the reactance of the line. The diagram of the whole setup is shown in figure 1.

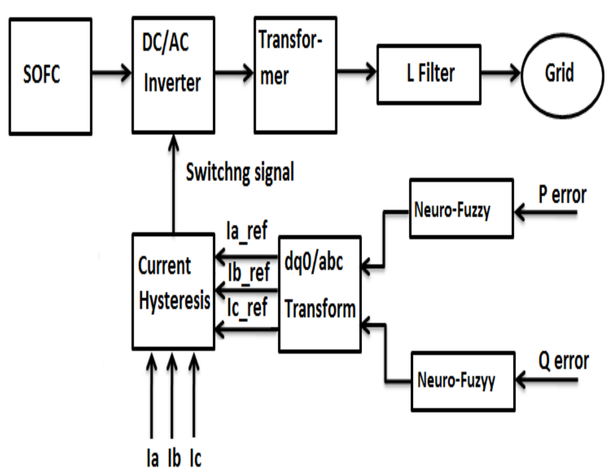

Figure 1 Schematic diagram of the proposed work.

Control Strategy for Grid Connected Inverter

The dq decouple control strategy is employed in this research paper. In this strategy, the active power is proportional to d-axis current while reactive power to q-axis current. Thus, the real power is controlled by the manipulation of d-axis current and reactive power is controlled by the manipulation of q-axis current. Neuro-Fuzzy receives the P and Q error which is the difference between the demand and power flowing in the bus. The controller output is given to the d-axis (direct axis). Similarly, Q error is given to the q-axis (quardrature axis).

The synchronously rotating currents Id and Iq are transformed into three phase currents by employing dq0/abc transformation. The mathematical representation of the aforementioned transformation is given in equation 6 [Diab et al., 2012].

The same strategy is applied for the PI and its performance is compared with Neuro-Fuzzy.

$$\begin{bmatrix} I_{a(ref)} \\ I_{b(ref)} \\ I_{c(ref)} \end{bmatrix} = \begin{bmatrix} 1 & 0 \\ \frac{-1}{2} & \frac{\sqrt{3}}{2} \\ \frac{-1}{2} & \frac{-\sqrt{3}}{2} \end{bmatrix} \begin{bmatrix} \cos\theta & -\sin\theta \\ \sin\theta & \cos\theta \end{bmatrix} \begin{bmatrix} I_d \\ I_q \end{bmatrix} \qquad (6)$$

Where I_{ref} are the three reference currents, $I_{a(ref)}$, $I_{b(ref)}$, and $I_{c(ref)}$ and I_{means} are the grid currents I_a, I_b *and* I_c.

Neuro-Fuzzy Network

The Neuro-Fuzzy [Nauck et al., 1997] is the fusion of Fuzzy logic and Neural networks. The total numbers of layers are four in this research work demonstrated in figure 2.

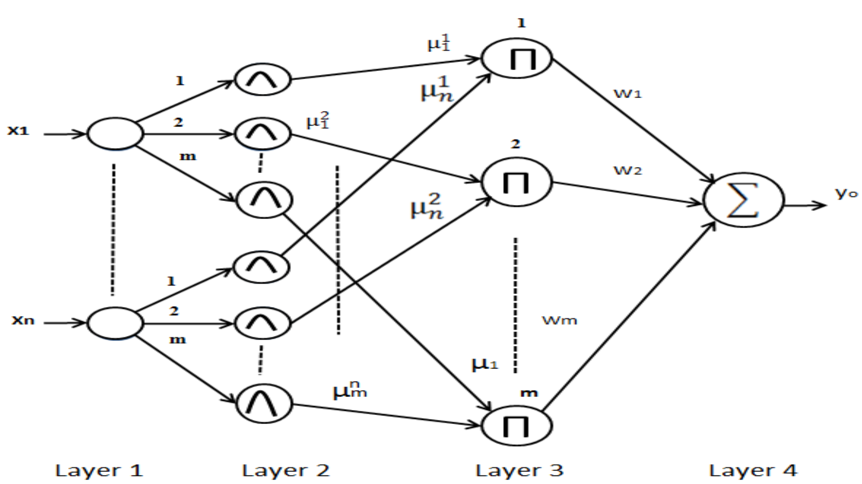

Figure 2 Fuzzy Neural network Architecture.

In the figure, Layer 1, layer 2, layer 3, and Layer 4 are the input, fuzzification, rule and defuzzification, respectively. . There are two rules in the algorithm, “If” is the antecedent part and “then” is the consequent part.

The rules defined can generally be expressed as equations 7.

$$\begin{aligned} &\text{Rule 1: If } A \text{ is } A_1 \text{ and } B \text{ is } B_1 \text{ then } y \text{ is } y_i \\ &\text{Rule 2: If } A' \text{ is } A_1' \text{ and } B' \text{ is } B_1' \text{ then } y' \text{ is } y_1' \end{aligned} \tag{7}$$

Standard Additive Model

Standard Additive Model, proposed by [Kosko, 1997], gets fuzzy inferences and is used for the approximation of fuzzy models as equation 8.

$$F(x) = Centroid\left(\sum_{i=1}^{m} h_i w_i(x) B_j\right) = \frac{\sum_{i=1}^{m} h_i w_i(x) V_i c_i}{\sum_{i=1}^{m} h_i w_i(x) V_i} = \sum_{i=1}^{m} p_i(x) c_i \tag{8}$$

In equation 8, h_i is the i_{th} weight.

The weight of the rule can be used to increase the usability and significance of the corresponding rule. In majority of the cases, it is considered as $h_1 \ldots\ldots\ldots h_m = 1$ and hence, the equal contributions of rules are considered. V_i represents the volume of the consequent, c_i represents the centroid of consequent, $w_i(x)$ represents the antecedent membership function and $p_i(x)$ represents the degree of fire:

- Parameters updating in SAM: This model updates its parameters by shifting the path of rules to extrema or bumps and covers the area.

  Adaptive SAM has a capability to search for the best approximation accuracy by finding out the most suitable rule structure. It is achieved by the adaptation or tuning the antecedents like membership functions, mean and variance with the consequent parameters like centroid and volume. Hence, the best approximation accuracy is obtained through tuning of the parameters.

  In adaptive SAM, the tuning of parameters can be obtained using supervised learning. The parameters of the SAM are estimated using the model equations and tuned by applying the gradient descent algorithm. The goal is to lower the square of error, equation 9.

$$E_k = \frac{1}{2}(y_k - t_k)^2 \tag{9}$$

The update process required for determining the fuzzy rules has a direct relation with the non-linearity of the output of the controllers. This non-linearity is tuned through altering the defined parameters that are position and spread of membership function. In short, the error is minimized by updating the parameters. There are different membership functions to be used as antecedent. In this research work, the function used is Gaussian and can be mathematically represented as equation 10.

$$w_j(x_i) = exp\left\{-\sum_{j=1}^{m}\left[\frac{x_i - m_{ij}{}^*}{\delta_{ij}}\right]^2\right\} \tag{10}$$

The means of the antecedent, centroid and volume can be derived by using chain rule. The equation of the mean can be derived as equations 11.

$$\frac{\partial E_k}{\partial_{m_{ij}}{}^*} = \frac{\partial E_k}{\partial F}\frac{\partial F}{\partial w_i}\frac{\partial w_i}{\partial m_{ij}{}^*}$$

$$m^*{}_{ij}(t+1) = m^*{}_{ij}(t) + 2 \propto ep_j(x)\left[c_j - F(x)\right]\frac{x - m^*{}_{ij}}{\delta_{ij}{}^2} \tag{11}$$

Similarly, the equation of variance of the antecedent part can be derived as equations 12.

$$\frac{\partial E_k}{\partial \delta_{ij}} = \frac{\partial E_k}{\partial F}\frac{\partial F}{\partial w_i}\frac{\partial w_j}{\partial \delta_{ij}}$$

$$\delta_{ij}(t+1) = \delta_{ij}(t) + 2\alpha ep_j(x)\left[c_j - F(x)\right]\frac{\left(x - m^*{}_{ij}\right)^2}{\delta_{ij}{}^3} \tag{12}$$

The equation of the centroid can be derived as equations 13.

$$\frac{\partial E_k}{\partial c_j} = \frac{\partial E_k}{\partial F}\frac{\partial F}{\partial c_j}$$

$$c_j(t+1) = c_j(t) + \alpha ep_j(x) \tag{13}$$

Similarly, the update equation of volume can be derived as equations 14.

$$\frac{\partial E_k}{\partial V_j} = \frac{\partial E_k}{\partial F}\frac{\partial F}{\partial V_j}$$
$$V_j(t+1) = V_j(t) + \propto e\left[c_j - F(x)\right]\frac{p_j(x)}{V_j} \quad (14)$$

While F represents the output.

- Back propagation based adaptive SAM: The learning process of adaptive SAM involves two steps: the forward pass and backward pass.

  In the first step, the current degree of fire of rules, the h_i's,their normalized values p_i's and the estimated output of fuzzy model F are calculated. Also, the current estimates $y_i{}^*(k)$, $m_{ij}{}^*$ and $\delta_{ij}(k)$ of unknown parameters $y_i{}^*(k)$, $m_{ij}{}^*$ and $\delta_{ij}(k)$ are used. Where $y_i{}^*(k)$ represent the consequent parameters having centroid and volume.

  In the second step, the current parameters estimates $y_i{}^*(k), m_{ij}{}^*$ and $\delta_{ij}(k)$ according to the learning rules, equations 11 a equations 14.

3. Results y Discussions

The set up consists of SOFC stack (rated at 50 kW), Power Conditioning Unit, Transformer, Filter, grid and Control units. The 50 kW is scaled at 1 p.u. The simulations are carried out at a constant temperature of the stacks at 1273 K. The real and reactive power delivered to the grid is shown in figures 3 and 4, which closely tracks the load profile. The slight gap, however, can be seen between the demand and power supplied by the SOFC based system. This gap is due to the time taken by the stacks to adjust chemical reaction and controller to minimize the error. The control strategy enables the SOFC based system to deliver both the power simultaneously which is shown in figure 5. The flow of real and reactive power is independent of each other.

The switching action and the time varying grid demand causes some harmonics in the output three phase voltage waveform which is shown in figure 6. This waveform is not only feasible for grid coupling but also affect the operating life of SOFC.

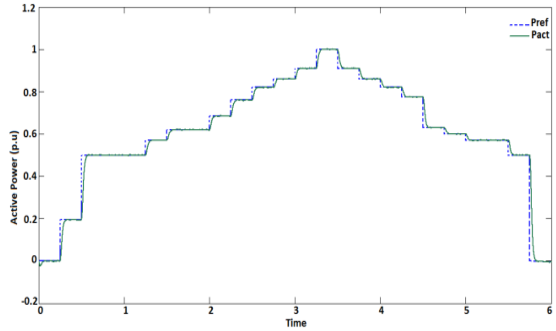

Figure 3 Tracking of active power demand of Grid.

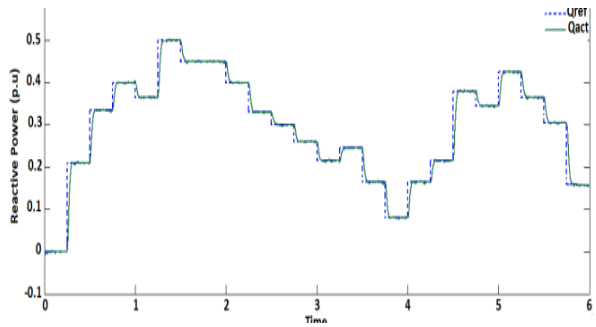

Figure 4 Tracking of reactive power demand of grid.

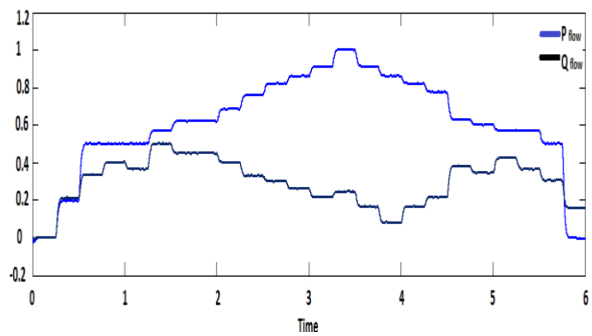

Figure 5 Independent flow of real and reactive power.

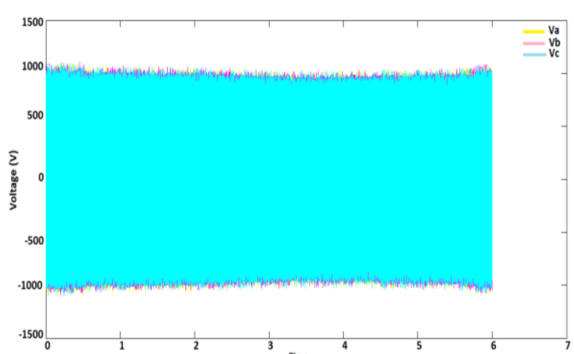

Figure 6 Unfiltered voltage waveform of VSI.

The L filter is connected between VSI and grid so as to remove the undesirables from output waveform of the inverter. The output waveforms of the voltage and its corresponding current of the VSI after employing L filter are shown in figure 7 and 8 respectively. The series inductor is working as a low pass filter which removes the harmonics thus keeping the waveform desirable for the load. The reference load profile is tracked by injecting the controlled current into the grid while keeping the peak of voltage at constant. The controller, control strategy and filter are successful in fulfilling the requirement of load and grid.

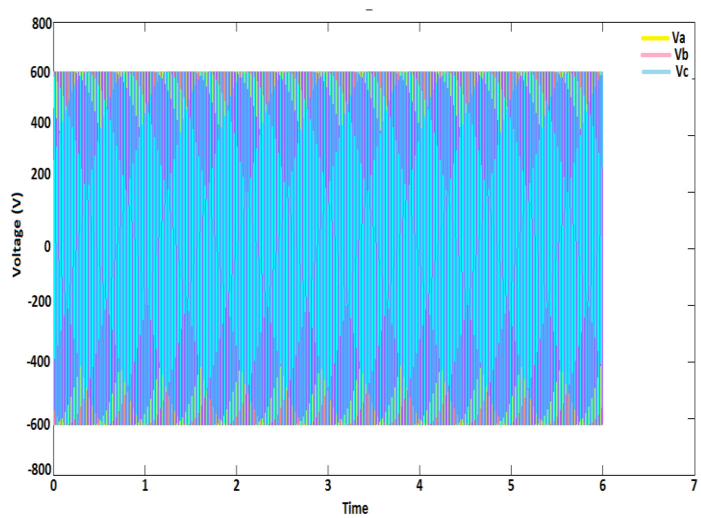

Figure 7 Filtered voltage waveform of VSI.

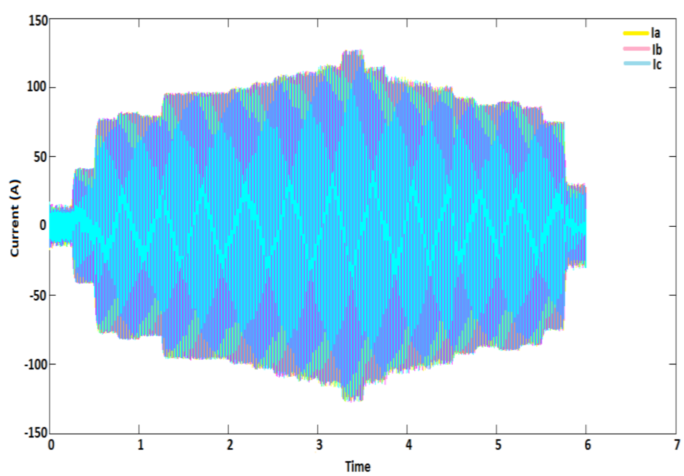

Figure 8 Current injected to the grid.

The above simulations are carried out using Neuro-Fuzzy controllers. Finally, the comparison between PI and Neuro-Fuzzy controller is shown in figure 9. It is shown for a short duration of 1 second with a step reference in order to visualize the performance of both controllers. Thus, it can be clearly seen in the figure that the Neuro-Fuzzy controller outperforms the PI in tracking the reference demand. Thus, Neuro-Fuzzy supersedes PI.

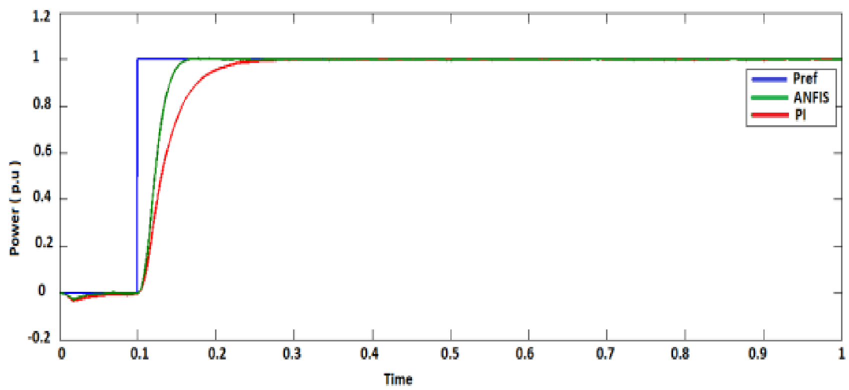

Figure 9 Performance comparison of Neuro-Fuzzy and PI for a step input.

5. Conclusion

In this research paper, the SOFC was coupled with the grid through the VSI and its corresponding control units. Two different controllers, Neuro-Fuzzy and PI, were tested for tracking the time-varying grid demand. It was found that both the controllers are capable in tracking the grid demand with the Neuro-Fuzzy being preferred for its better performance. Furthermore, with the use of L filter, the output three phase voltage waveform of the VSI is free of harmonics, and thus feasible for feeding into the grid. The strategy proposed in this work can be exploited in effectively coupling the SOFC with the grid. As a future work, the strategy needs to be tested for the higher ratings of power, however.

6. Bibliography and References

[1] Bhuyan, K. C., Mahapatra, K. K., An intelligent control of solid oxide fuel cell voltage, 2011 International Conference on Power and Energy Systems (ICPS), pp.1,6, 22-24, December 2011.

[2] Asadi, A., Mahmud, F., Moein, M, Techno-economic considerations on distributed generations (DGs) planning studies in power distribution systems, 2014 19th Conference on Electrical Power Distribution Networks (EPDC), vol., no., pp.82,87, 6-7, May 2014.

[3] Diab, H., El-Helw, H., Talaat, H., Intelligent Maximum Power Tracking and Inverter Hysteresis Current Control of Grid-connected PV Systems, IEEE 2012, International Conference on advances in Power Conversion and Energy Technologies (APCET), pp. 1-5, 2-4, Aug. 2012.

[4] Kang, H., Qingli, S., Zhengqui, W., Discussion on advantages and disadvantages of distribution generation connected to grid, IEEE 2011, International Conference on Electrical and Control Engineering (ICECE), 10.1109/ICECENG, pp. 170-173, 2011.

[5] Khan, Z. W., and Khan, S., Analyzing the impacts of Distributed Generation on power losses and voltage profile, 2015 International Conference on Emerging Technologies (ICET), Peshawar, pp. 1-4, 2015.

[6] Kosko, B., Fuzzy Engineering. Upper saddle River, NJ: Prentice-Hall, 1997.

[7] Mekhilef, S., Saidur, R., & Safari, A, Comparative study of different fuel cell technologies, Renewable and Sustainable Energy Reviews, pp.981-989, 2012.

[8] Nauck, D., Klawon, F., Kruse, R., Foundation of Neuro-Fuzzy Systems, J. Wiley and sons, 1997.

[9] Vaishampayan, V., Vangari, A., Shah, J., Challenges and opportunities of affordable Fuel Cell for distributed generation, 1st International Conference on Non Conventional Energy (ICONCE), 10.1109/ICONCE, 6808734, pp. 319-323, 2014.